A simple, flexible and generic deterministic approach to uncertainty quantifications in non linear problems : application to fluid flow problems

R. Abgrall

September 22, 2008

Abstract

This paper deals with the computation of some statistics of the solutions of linear and non linear PDEs by mean of a method that is simple and flexible. A particular emphasis is given on non linear hyperbolic type equations such as the Burger equation and the Euler equations.

Given a PDE and starting from a description of the solution in term of a space variable and a (family) of random variables that may be correlated, the solution is numerically described by its conditional expectancies of point values or cell averages. This is done via a tessellation of the random space as in finite volume methods for the space variables. Then, using these conditional expectancies and the geometrical description of the tessellation, a piecewise polynomial approximation in the random variables is computed using a reconstruction method that is standard for high order finite volume space, except that the measure is no longer the standard Lebesgue measure but the probability measure. Starting from a given scheme for the deterministic version of the PDE, we use this reconstruction to formulate a scheme on the numerical approximation of the solution.

This method enables maximum flexibility in term of the PDE and the probability measure. In particular, the scheme is non intrusive, can handle any type of probability measure, even with Dirac terms. The method is illustrated on ODEs, elliptic and hyperbolic problems, linear and non linear.

Contents

1 Introduction

We are interested in solving linear and non linear PDE, such as

$$\begin{array}{l} \dfrac{\partial u}{\partial t} + \dfrac{\partial f(u)}{\partial x} = \nu \dfrac{\partial^2 u}{\partial x^2} + S(x) \qquad\qquad t > 0, x \in \mathbb{R} \\ \text{Initial and/or boundary conditions} \end{array} \tag{1}$$

with $\nu \geq 0$ and S is a source term. Examples are given by a transport equation with $f(u) = au, S = 0$, the Burgers equation with $f(u) = \frac{1}{2}u^2$, the heat equation where $f = 0$ or even a Laplace equation where $f = 0$ and a time independent solution. Of course, in each case, the boundary conditions have to be adapted to the case under study.

In this paper, we assume in addition that the initial condition is a random variable $u_0 := u_0(x, \omega)$ where $\omega \in \Omega$ a probabilistic space. We assume that $u(\ .\ , \omega)$ has a known distribution law $d\mu$ which may or may not have a density. Examples are given by the uniform distribution, the Gaussian distribution, of a combination of a pdf with a density with Dirac-like distributions. In that case there is no density. In this work, we assume to know the pdf. The problem of knowing the distribution law of the solution of (1) is a difficult problem in general which is still open up to our knowledge.

There are many situations where one wants to estimate some statistics on the solution of a PDE. Consider the flow around an aircraft for example. The boundary conditions (inflow mach number, Reynolds number, some geometrical parameters) may only be known approximately either in a nozzle flow or a true flight. In hyper-sonics, the equation of state or the viscous model play an important role and they are sometimes known very approximately. The same is true for multiphase flows. One may also wish to "extrapolate" experimental results which are partialy known to flow conditions that are not contained in the experimental data base : what is the confidence one may have ? The question is not only to know the sensitivity of the solution of (1), but also to to understand the importance (i.e. the weight) of these variations. In other terms, assuming the likely-hood of relative variations, how can we weight their influence on the solution ?

The aim of this paper is to propose a general method which enables to compute (approximations of) the statistics of the exact solution with the smallest possible modification of an existing code. In particular we are interested in developing general purpose methods able to easily handle, with little or no code/scheme modification, the following list:

1. the pdf is general and may change either in time or through some optimisation loop for example,

2. the pdf may or may have a density, may or may be not compactly supported, or can be known only trough an histogram,

3. The initial solution may depend on several correlated or uncorrelated random variables.

4. no modification of the code has to be done when one changes the pdf,

5. as little as possible modification of an existing deterministic code/method is needed.

Namely, when one approximates (1) or more complex conservation systems, the coding effort is put on the spatial discretisation, the approximation of the flux and the time approximation.

The problem (1) is a very crude approximation of the above mentioned problem. Our aim is to develop a general methodology that could easily be extended to these more complex physical problems.

In most engineering situations, the numerical method is at most second order accurate. Saying this, we have in mind the case of a non linear problem of hyperbolic type or possibly with second order terms but which role is significant only in a small part of the computational domain. The prototype example is again (1) with $\nu << 1$. In engineering applications, this is the Navier Stokes equations. In these cases, since deterministic methods are generally second order accurate in time and space, our belief is that there is no need to have a method able to compute statistical quantities with an extremely high accuracy. The best would be to have a method where the dominant source of error comes from the deterministic method. The aim of this paper is to propose a method that is able to combine all these requirements.

The paper is organised as follow. First we review several existing techniques. In a second section, from several computational remarks, we propose a general framework to achieve our goal. This framework is illustrated by several examples, ranging from standard ODEs, to Euler equations, via an elliptic problem and several scalar hyperbolic problems. Every time this is possible, error with respect to the exact solution are given.

2 Review of existing techniques

In many cases, the definition of the physical problem is not fully known. This may be the case for several reasons including:

- The geometry may be known only partially. Imagine that the body surface is rough, one can certainly parametrize the roughness by some random parametrisation

- The boundary conditions may be partially known only, for example in the case of fluctuations of some parameters,

- Some constants in the model can be uncertain, think for example of a turbulence model or the parametrization of the equation of state. This is a very important practical problem for industry.

In each case, even if the model, hence the numerical method ..., suffers from deficiencies, there is still a need to compute and simulate !

In order to tackle this issues, there are currently several techniques available in the engineering community, and this is a very active research topic.

One technique relies on polynomial chaos expansion. Assuming that the random inputs data which depends on space $x \in A \subset \mathbb{R}^d$ and a a random parameter, say the boundary conditions to fix ideas, is defined on a probabilistic space $(\Omega, \mathcal{A}, P)$ and has a finite variance, we can define the covariance matrix

$$C(x,y) = E(X(x,.)X(y,.)), \text{ for } x, y \in A.$$

If f_k is the k–th eigenfunction

$$\int_A C(x,y) f_k(y) dy = \lambda_k f_k(x),$$

one can write the Karhunen-Loève expansion of X,

$$X(x,\omega) = \sum_{k=0}^{\infty} \sqrt{\lambda_k} f_k(x) \zeta_k(\omega) \tag{2}$$

where the ζ_k are uncorrelated Gaussian random variables. Then, following [1], one can expand the solution of (1) as

$$\begin{aligned} u(t,x,\omega) = a_0\Gamma_0 &+ \sum_{i_1=1}^{\infty} a_{i_1}\Gamma_1(\zeta_1(\omega)) + \sum_{i_1=1}^{\infty}\sum_{i_2=1}^{\infty} a_{i_1 i_2}\Gamma_2(\zeta_1(\omega),\zeta_2(\omega)) \\ &+ \dots \\ &+ \sum_{i_1=1}^{\infty}\sum_{i_1=1}^{\infty}\cdots\sum_{i_k=1}^{\infty} a_{i_1 i_2 \dots i_k}\Gamma_k(\zeta_1(\omega),\zeta_2(\omega),\dots,\zeta_k(\omega)) \\ &+ \dots \end{aligned} \tag{3}$$

The functions Γ_k are defined by

$$\Gamma_k(\zeta_1,\zeta_2,\dots,\zeta_k) = (-1)^k e^{\zeta\cdot\zeta^T} \frac{\partial^k e^{-\zeta\cdot\zeta^T}}{\partial\zeta_1\dots\partial\zeta_k}.$$

The idea is, after truncation both in the random input and (3), to introduce this relation into (1), then to use a spectral method (because of the form of the Γ_k). There are other versions of this polynomial chaos, see for example [2, 3].

In our opinion, there are at least three drawbacks to this approach. First, it is not clear at all what should be the right truncation level in the expansion (3), see for example [4]. Second, if one has a good numerical method to solve one problem, the numerical strategy has to be revisited from A to Z to go to another one, which is not acceptable from an engineering point of view. It is also not clear how to handle discontinuities in the formulation. The last one is that if one changes the structure of the input random function, every thing has to be restarted from scratch. This is the case in particular when new informations are introduced to the system.

The second problem of the previous approach, that the method is intrusive, can be tackled by a method which is in between the spectral expansion that has been sketched above and the Monte

Carlo method. One chooses a "good" set of random realisations and one run the baseline numerical scheme for these random parameters. Since the output of the whole computation is to evaluate expectation of a functional f of the the solution, say the pressure distribution to fix ideas, these functional depend on $\zeta_1, \ldots, \zeta_N$. The random parameters are chosen such that the expectancy

$$E(f) = \int_\Omega f(\zeta_1, \ldots, \zeta_N) d\mu$$

can be evaluated easily with a good accuracy. This amounts to find quadrature points for this integral. These quadrature points are related in general to zeros of some orthogonal polynomials. The curse of dimensionality can be tackled by mean of the Smolyak quadrature formula, for example. This path has been explored by several researchers, see for example [5].

In our opinion, one of the weakness of this technique is that if the probability density functions are not smooth enough – this may occur in some combustion problems, see [4, 6] for example–, the convergence of the integral may be very slow.

In both cases, an other major drawback is the following: the pdf is in general not known, so that the whole process collapses. The numerical procedure may be one part of a more general loop in which a learning process is implemented, via some optimisation loop for example. Clearly, once the expansion (2) has been chosen, there is no space for any learning process so that the expected results of the whole methodology can be disappointing. How can we construct a numerical method, able to handle true fluid problems, for which a learning process can be implemented ?

3 Principles of the method

3.1 Some computational remarks

Let $d\mu$ a probability measure and X a random variable defined on the probability space $(\Omega, d\mu)$. Assume we have a decomposition of Ω by non overlapping subsets Ω_i, $i = 1, N$ of strictly positive measure:

$$\Omega = \cup_{i=1}^N \Omega_i.$$

We are given the conditional expectancies $E(X|\Omega_i)$. Can we estimate for a given f, $E(f(X))$? We assume $X = (X_1, \ldots, X_n)$

The idea is the following: For each Ω_i, we wish to evaluate a polynomial $P_i \in \mathbb{R}^n[x_1, \ldots, x_n]$ of degree n such that

$$E(X|\Omega_j) = \frac{\int_{\mathbb{R}^n} 1_{\Omega_j}(x_1, \ldots, x_n) P(x_1, \ldots, x_n) d\tilde{\mu}}{\mu(\Omega_i)} \qquad \text{for } j \in \mathcal{S}_i \tag{4}$$

where $d\tilde{\mu}$ is the image of $d\mu$ and $\mathcal{S}_i$ is a stencil associated to Ω_i. [1]

This problem is reminiscent of what is done in finite volume schemes to compute a polynomial reconstruction in order to increase the accuracy of the flux evaluation thanks the MUSCL extrapolation. Among the many references that have dealt with this problem, with the Lebesgue measure

[1] for example $d\mu$ is the sum of a Gaussian and a Dirac at x_0,

$$\int_{\mathbb{R}^n} P(x) d\tilde{\mu} = \alpha \frac{1}{\sqrt{2\pi\sigma}} \int_{\mathbb{R}} P(x) e^{-\frac{(x-m)^2}{2\sigma}} dx + (1-\alpha) P(x_0)$$

$dx_1 \dots dx_n$, one may quote [7] and for general meshes, one may quote [8, 9]. A systematic method for computing the solution of problem (4) is given in [10].

Assume that the stencil $\mathcal{S}_i$ is defined, the technical condition that ensure a unique solution to problem (4) is that the Vandermonde–like determinant (given here for one random variable for the sake of simplicity)

$$\Delta_i = \det \Big(E(x^l|\Omega_j) \Big)_{0 \le l \le n, j \in \mathcal{S}_i}.$$

is non zero. In the case of several random variable, the exponent l above is replaced by a multi–index.

Once the solution of (4) is known, we can estimate

$$E(f(X)) \approx \sum_{j=1}^{N} \int_{\mathbb{R}^n} 1_{\Omega_j}(x_1, \dots, x_n) f\Big(P(x_1, \dots, x_n) \Big) d\tilde{\mu}.$$

We have the following approximation results : if $f \in C^p(\mathbb{R}^n)$ with $p \ge n$ then

$$\Big| E(f(X)) - \sum_{j=1}^{N} \int_{\mathbb{R}^n} 1_{\Omega_j}(x_1, \dots, x_n) f\Big(P(x_1, \dots, x_n) \Big) d\tilde{\mu} | \le C(\mathcal{S}) \max_j \big[\mu(\Omega_j)^{\frac{p+1}{p}} \big]$$

for a set of regular stencil which proof is straightforward generalisation of the approximation results contained in [11].

In all the practical illustrations, we will use only one or two sources of uncertainty even though the method can be used for any number of uncertain parameters, this leading to other known problems such that the curse of dimensionality. The space Ω is subdivided into non overlapping measurable subsets. In the case of one source of uncertainty, the subsets can be identified, via the measure $d\mu$, to N intervals of $\mathbb{R}$ which are denoted by $[\omega_j, \omega_{j+1}]$. The case of multiple sources can be considered by tensorisation of the probabilistic mesh. This formalism enables to consider correlated random variables, as we show later in the text.

Let us describe in details what is done for one source of uncertainties. In the cell $[\omega_i, \omega_{i+1}]$, the polynomial $P_{i+1/2}$ is fully described by a stencil $\mathcal{S}_{i+1/2} = \{i + 1/2, i_1 + 1/2, \dots\}$ such that in the cell $[\omega_j, \omega_{j+1}]$ with $j + 1/2 \in \mathcal{S}_{i+1/2}$ we have

$$E(P_{i+1/2}|[\omega_j, \omega_{j+1}]) = E(u|[\omega_j, \omega_{j+1}]).$$

It is easy to see that there is a unique solution to that problem provided that the elements of $\{[\omega_j, \omega_{j+1}]\}_{j+1/2} \in \mathcal{S}_{i+1/2}$ do not overlap, which is the case. In the numerical examples, we consider three reconstruction mechanisms :

- a first order reconstruction: we simply take $\mathcal{S}_{i+1/2} = \{i + 1/2\}$ and the reconstruction is piece-wise constant,
- a centered reconstruction: the stencil is $\mathcal{S}_{i+1/2} = \{i - 1/2, i + 1/2, i + 3/2\}$ and the reconstruction is piece–wise quadratic. At the boundary of Ω, we use the reduced stencils $\mathcal{S}_{1/2} = \{1/2, 3/2\}$ for the first cell $[\omega_0, \omega_1]$ and $\mathcal{S}_{N-1/2} = \{N - 1/2, N - 3/2\}$ for the last cell $[\omega_{N-1}, \omega_N]$, i.e. we use a linear reconstruction at the boundaries.

- An ENO reconstruction : for the cell $[\omega_i, \omega_{i+1}]$, we first evaluate two polynomials of degree 1. The first one, p_i^-, is constructed using the cells $\{[\omega_{i-1}, \omega_i], [\omega_i, \omega_{i+1}]\}$ and the second one, p_i^+, on $\{[\omega_i, \omega_{i+1}], [\omega_{i+1}, \omega_{i+2}]\}$. We can write (with $\omega_{i+1/2} = \frac{\omega_i + \omega_{i+1}}{2}$)

$$p_i^+(\xi) = a_i^+(\xi - \omega_{i+1/2}) + b_i^+ \text{and } p_i^-(\xi) = a_i^-(\xi - \omega_{i+1/2}) + b_i^- .$$

  We choose the least oscillatory one, i.e. the one which realises the oscillation $\min(|a_i^+|, |a_i^-|)$. In that case, we take a first order reconstruction on the boundary of Ω.

Other choices are possible such as WENO-like interpolants. Again, the case of multiple source of uncertainties can be handled by tensorisation.

3.2 A general strategy

Let us start from a PDE of the type

$$\mathcal{L}(u, \omega) = 0 \tag{5}$$

defined in a domain K of $\mathbb{R}^d$, subjected to boundary conditions. Since the discussion of this section is formal, we put the different boundary conditions of the problem in the symbol $\mathcal{L}$. The term ω is a random parameter, i.e an element of a set Ω equipped with a probability measure $d\mu$. In (5), the uncertainty is weakly coupled with the PDE, i.e. ω does not depend on any space variables. However, the measure $d\mu$ may depend on some space variable. The examples we have in mind are such that for a given realisation $\omega_0 \in \Omega$, $\mathcal{L}(u, \omega_0) = 0$ is a "standard" PDE, such as the Laplace equation, Burgers equation, the Navier Stokes equations, etc. To make things even more clear, and to give an example, let us consider the heat equation

$$\frac{\partial T}{\partial t} = \text{div } (\kappa \nabla T) + S(t, x), \qquad t > 0, x \in K \subset \mathbb{R}^d$$

with Dirichlet boundary conditions

$$T = g \text{ on } \partial K$$

and initial conditions

$$T(x, 0) = T_0(x).$$

In this example, κ, the source term S, the boundary condition g, the domain K and the initial condition T_0 may be random. For any realisation of Ω, we are able to solve the heat equation by some numerical method. What we are looking for is, for example, statistics on the approximate solution T when ω follows a given probability law.

We are given a numerical method for solving $\mathcal{L}(u, \omega_0) = 0$, say

$$\mathcal{L}_h(u_h, \omega_0) = 0.$$

for any $\omega_0 \in \Omega$

This gives birth to a method for solving (5) that we denote $\mathcal{L}_h(u_h, \omega) = 0$. Once this is done, we have to discretise the probability space Ω: we construct a partition of Ω, i.e. a set of Ω_j, $j = 1, \ldots, N$ that are mutually independent

$$\mu(\Omega_i \cap \Omega_j) = 0 \text{ for any } i \neq j$$

and that cover Ω

$$\Omega = \cup_{i=1}^{N} \Omega_i.$$

We assume $\mu(\Omega_i) > 0$ for any i. Our problem is to estimate $E(u_h|\Omega_j)$ from $\mathcal{L}(u, \omega) = 0$.

For example, if an iterative technique is used for solving the deterministic problem, say

$$u_h^{n+1} = \mathcal{J}(u_h^n),$$

this leads to

$$u_h^{n+1}(\omega) = \mathcal{J}(u_h^n, \omega),$$

so that

$$E(u_h^{n+1}|\Omega_j) = E(\mathcal{J}(u_h^n)|\Omega_j).$$

In the examples we have in mind, the operator $\mathcal{J}$ is a succession of additions, multiplications and function evaluations. The average conditional expectancies, as we have explained in the previous section, enable to compute approximations of the average conditional expectancies of any functional, so that the evaluation of $E(\mathcal{J}(u_h^n)|\Omega_j)$ can be done in practice: we are able to construct a sequence $\left(E(u_h^{n+1}|\Omega_j)\right)_{n\geq 0}$. *If this sequence converges in some sense*, the limit is the sought solution.

This example is also useful for *clarifying what we are not looking for*. It may well be that the functional coming into $\mathcal{J}$ depend on several instance of u_h, for example the value of u_h at several mesh point locations. In our method, we need that the probability law be the same all over the computational domain K, or we would need joint probabilities between the various variables coming into play. If this is doable in theory, we do not believe it is doable in practice. Moreover, for all the examples we have in mind, it is reasonable to assume that the probability law is the same all over the computational domain.

In the next sections, we provide examples of realisations of this program on elliptic, parabolic and hyperbolic equations with some non linear examples.

4 Example of an ODE

Our first example is a simple ODE equation with initial condition,

$$\begin{aligned} \frac{du}{dt} &= f(u,t) \\ u(x, t=0, \omega) &= u_0(x, \omega) \end{aligned} \tag{6}$$

where f is assumed to be smooth enough for having a unique solution. Here, we assume that f is C^1, but this assumption is certainly too strong and could be lower by a deeper analysis, This is not our point here.

The equation (6) is discretised, for any ω, by an ODE solver. To make things simple, but without loss of generality, assume that we use the first order Euler forward method

$$u^{n+1}(\omega) = u^n(\omega) - \Delta t\ f(u^n(\omega), t_n).$$

Then we have, for any Ω_i

$$E(u^{n+1}|\Omega_i) = E(u^n|\Omega_i)) - \Delta t\ E(f(u^n, t_n)|\Omega_i). \tag{7}$$

The problem is to evaluate $E(f(u^n, t_n)|\Omega_i)$. This can be done via a numerical quadrature thanks to the reconstruction we have developed in section 3.1. Let us give an example, say

$$f(u,t) = \begin{cases} u(u-\frac{1}{2})(1-u) & \text{if } u \in [\frac{1}{4}, \frac{3}{4}] \\ 0 & \text{else.} \end{cases} \tag{8}$$

In that example,

$$u_\infty = \lim_{t \to +\infty} u(t) = \begin{cases} u_0 & \text{if } u_0 < \frac{1}{4} \\ \frac{1}{2} & \text{if } \frac{1}{4} \le u_0 < \frac{3}{4} \\ u_0 & \text{if } u_0 > \frac{3}{4}. \end{cases}$$

From this, we see easily that if u_0 is random with probability law $d\mu$, the repartition function of u_∞ is

$$\Phi(u) := P(\omega | u_\infty(\omega) \le u) = \begin{cases} P(s \le u) & \text{if } u < \frac{1}{4} \\ P(s \le \frac{1}{4}) & \text{if } \frac{1}{4} \le u < \frac{1}{2} \\ P(s \le \frac{3}{4}) & \text{if } \frac{1}{2} \le u < \frac{3}{4} \\ P(s \le u) & \text{if } u \ge \frac{3}{4} \end{cases}$$

Take the scheme is (7) with a third order reconstruction (with a centered stencil) except on the boundaries of Ω where, if Ω_0 and Ω_N are the boundary cells, we take the following stencils

- for Ω_0, $\mathcal{S} = \{0, 1\}$,
- for Ω_N, $\mathcal{S} = \{N-1, N\}$.

The results are independent of the high order reconstruction formula because the solution limit value $u_\infty = \frac{1}{2}$ is stable.

A third order quadrature Gaussian formula is used in the case of a probability with a density

$$\int_a^b f(x)dx \approx \frac{b-1}{2}\Big(f\big(\frac{a+b}{2} + \theta(b-a)\big) + f\big(\frac{a+b}{2} - \theta(b-a)\big)\Big), \qquad \theta = \frac{1}{\sqrt{3}}.$$

An optimal 6th order Gauss quadrature formula could have been used, but since the time stepping is only first order, and since the numerical examples we consider are steady, there is no need to deal with optimally order quadrature formula. When there is no density, for example if $d\mu = f dx + C\delta_a$, the regular part of μ is dealt with the previous formula, and the singular one by an ad hoc one.

In order to illustrate the method, we consider three pdfs. Here, we set $d\mu = f(x)dx$

- a uniform distribution :
$$f(x) = 1_{[0,1]},$$
- A Gaussian distribution on $[-2, 2]$ with 0 mean and variance $\sigma = 1$,
$$f(x) = \frac{e^{-x^2/2}}{\int_{-3}^{3} e^{-s^2/2} ds},$$
- A Poisson distribution on $[0, 2]$,
$$f(x) = 1_{[0,2]} \frac{e^{-x}}{1 - e^{-2}},$$

,

In these example, any of the three reconstruction methods presented in section 3.1 works fine. We have chosen the centered one for the numerical illustration since it is a priori the most accurate one.

We show how the method approximates the values $P(s \leq \frac{1}{4})$ and $P(s \leq \frac{1}{2})$. We have chosen a very crude way of the repartition function of the random variable u_∞,

$$\Psi(U_\infty) \approx \sum_j P(s \in [\omega_j, \omega_{j+1}] \text{such that } u_\infty(s) \leq U_\infty).$$

This explains the staircase like behavior of the curves of Figure 2 where we have displayed the results for these three pdfs. This method is accurate however when 1/4 and 1/2 are mesh points in the probability space, in which case the only approximation holds on the quadrature defining the terms $P(s \in [\omega_j, \omega_{j+1}])$. We see on figure 1 that the method has the accuracy of the quadrature formula (fourth order accurate) when the probability mesh meet this condition; this test has been conducted with the Gaussian pdf. Other results obtained for the other pdfs and 101 points are displayed in Table 1.

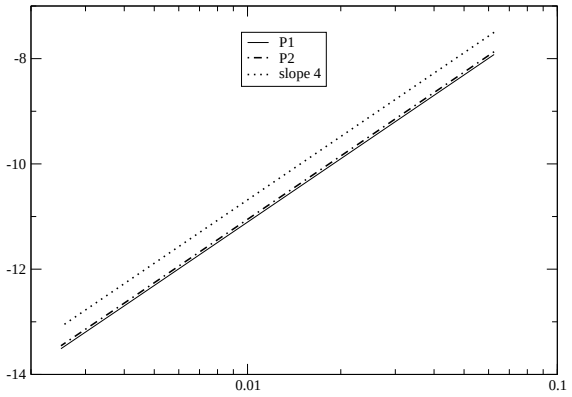

Figure 1: Error in the evaluation of $\Psi(U_\infty)$ when $U_\infty \in]\frac{1}{4}, \frac{1}{2}[$ and $U_\infty \in]\frac{1}{2}, \frac{3}{4}[$ for optimal meshes.

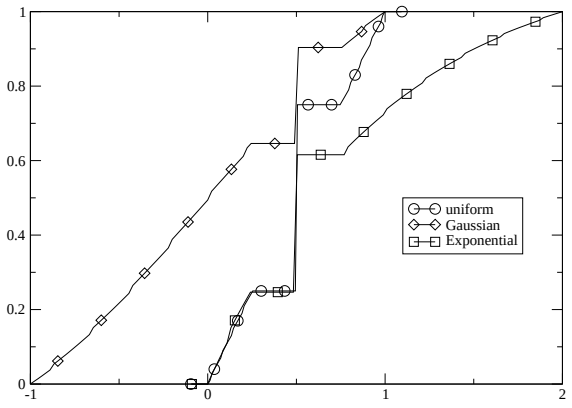

Figure 2: Repartition function for the EDO (8) and the three pdf.

The error between the exact and numerical results for $P_1 = \Psi(\frac{1}{4})$ and $P_2 = \Psi(\frac{3}{4})$ in the case of the Gaussian distribution is displayed in Figure 1.

$\Psi(U_\infty)$	Uniform	Gauss	Poisson
$U_\infty \in]\frac{1}{4}, \frac{1}{2}[$	$\frac{1}{2}$	$\frac{\mathrm{erf}(1/4) - \mathrm{erf}(-1)}{\mathrm{erf}(1) - \mathrm{erf}(-1)}$	$\frac{1 - e^{-1/2}}{1 - e^{-2}}$
exact		$\approx 0.64458450997090083670$	≈ 0.2558207969
computed	0.25	0.644584509951823	0.246768643147764
$U_\infty \in]\frac{1}{2}, \frac{3}{4}[$	$\frac{3}{4}$	$\frac{\mathrm{erf}(3/4) - \mathrm{erf}(-1)}{\mathrm{erf}(1) - \mathrm{erf}(-1)}$	$\frac{1 - e^{-3/4}}{1 - e^{-2}}$
exact		$\approx 0.90043482545390904212$	0.6102173907
Computed	0.75	0.900434825432325	0.615653168991007

Table 1: Numerical values found for Ψ at the critical points. There are 101 points in the probability mesh.

At first glance, it might look strange that a centered reconstruction works well for a problem that admits discontinuous results. It is well known that such reconstruction suffers from a Gibbs–like phenomena. However here, the problem a bit special. The two solutions $u_\infty = 0$ and $u_\infty = 1$ are unstable and the way we have proceed avoid them. We have kept only the the stable one $u_\infty = \frac{1}{2}$. More over, if $u \in [\frac{1}{4}, \frac{3}{4}]$ we have $u_\infty = u_0$ and the initial condition is linear. Thus the reconstruction is exact here. If any oscillation develop (i.e. when in the transient, we are out are out of $[\frac{1}{4}, \frac{3}{4}]$), the solution will be attracted to the closest stable limit solution, i.e. $u_\infty = \frac{1}{2}$. two possible cases

5 Example of an elliptic problem

As an illustration, we consider the simple problem

$$\begin{array}{ll} (\kappa(x,\omega)u')' = 0 & , x \in]0,1[\\ u(0) = 0 & , u(1) = 1 \end{array} \tag{9}$$

where $\omega \in \Omega$ is random with a given pdf, and $\kappa(x,\omega) > \kappa_0 > 0$ on $]0,1[\times\Omega$ which solution is

$$u(x,\omega) = \frac{\int_0^x \frac{1}{\kappa(x,\omega)} dx}{\int_0^1 \frac{1}{\kappa(x,\omega)} dx}.$$

Equation (9) is approximated on the mesh $x_i = i\Delta x$, $i = 0, \ldots, N$ by (the mesh is uniform)

$$\begin{array}{l} \kappa_{i+1/2}(u_{i+1} - u_i) - \kappa_{i-1/2}(u_i - u_{i-1}) = 0 \quad 1 \le i \le N-1 \\ u_0 = 0, u_N = 1 \end{array}$$

that is

$$\begin{array}{r} u_i = \dfrac{\kappa_{i+1/2}u_{i+1} + \kappa_{i-1/2}u_{i-1}}{\kappa_{i+1/2} + \kappa_{i-1/2}} \\ u_0 = 0, u_N = 1, \end{array} \tag{10}$$

and $\kappa_{j+1/2} := \kappa(x_{j+1/2}, \omega)$.

The rest of the method is similar, and we have used the same quadrature formula as in the previous paragraph.

In the numerical examples, we have chosen

$$\kappa(x,\omega) = 4(x-0.5)^2 + 0.33\cos\left(\frac{2\pi\omega}{4}\right)(x-0.5) + 0.01$$

Here $\kappa \geq 0.003$. The pdf is a Gaussian distribution with mean 0.5 and variance 0.5.

In figure 3, we show the result obtained for 101 points in the space direction and 21 points in the probability direction. Again a centered reconstruction is used.

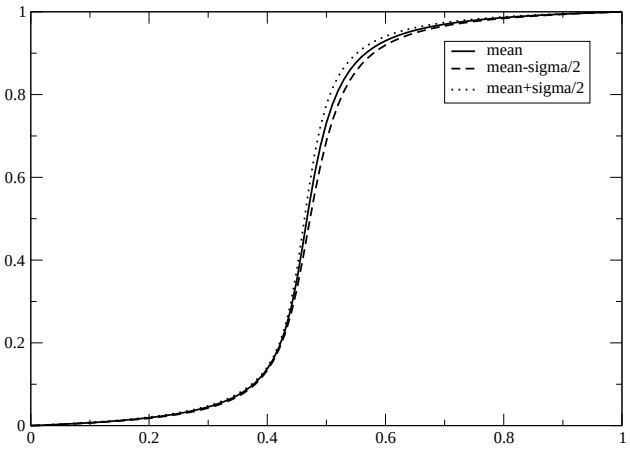

Figure 3: Mean and variance for 101 points in the space direction and 21 points in the probability direction.

The exact solution is

$$u(x,\omega) = \frac{\arctan\left(\frac{x-\varphi}{\delta}\right) + \arctan\left(\frac{\varphi}{\delta}\right)}{\arctan\left(\frac{1-\varphi}{\delta}\right) + \arctan\left(\frac{\varphi}{\delta}\right)}$$

with

$$\varphi = 0.5 - \frac{0.33}{8}\cos(2\pi\omega), \qquad \delta = \sqrt{0.0025 - \left(\frac{0.35}{8}\right)^2\cos^2\left(\frac{2\pi\omega}{4}\right)}.$$

so that it is easy to estimate the L^∞ and L^2 errors of the mean and variance. This is done on figure 4. The results are second order accurate with respect to the space variable. We see also that the results are almost independent of the discretisation in the probability direction. "Converged" results are obtained already with 9 cells in the probability direction.

6 Example of the convection and Burgers equations

Our next example is the Burgers equation (1). In order to illustrate the strategy, we start from a MUSCL type predictor–corrector second order scheme.

$$\begin{array}{ll} \dfrac{\partial u}{\partial t} + \dfrac{\partial f(u)}{\partial x} = 0 & t > 0, x \in \mathbb{R} \\ u(x,t) = u_0(x) & x \in \mathbb{R} \end{array} \tag{11}$$

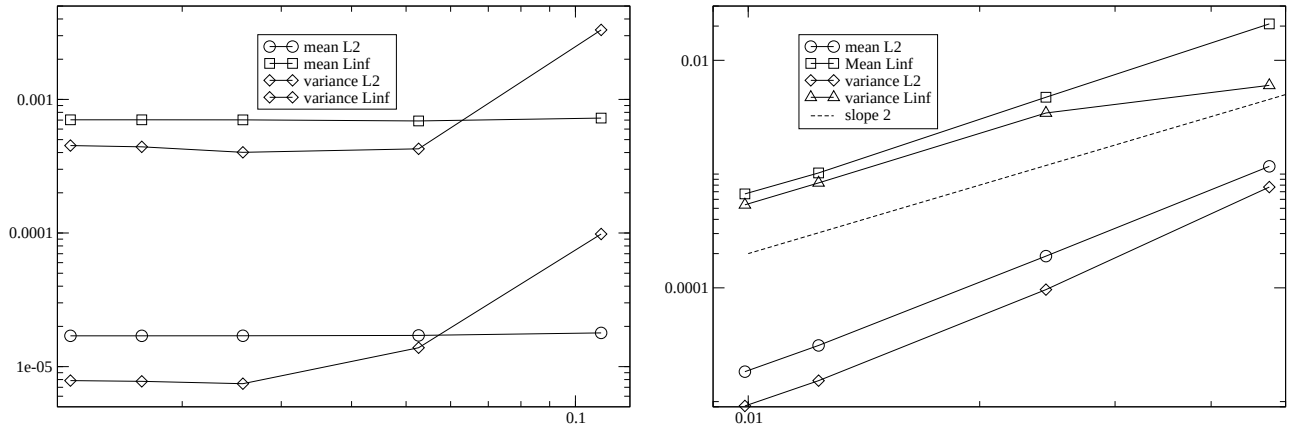

Figure 4: Errors in the mean and variance. (a) represents the error for a fixed space discretisation ($\Delta x = 10^{-2}$) and a varying probability discretisation (from 10 to 80) points. (b) represents the error for a fixed probability discretisation (50 points) and a varying space discretisation (from 20 to 101 points). The slope -2 is represented. The results are obtained with a centered recontruction.

with periodic boundary conditions on $[0, 2\pi]$. For the convection problem, we take $f(u) = u$ and for the Burgers equation, we take $f(u) = u^2/2$. The interval $[0, 2\pi]$ is subdivided into equally spaced sub–intervals $[x_{i-1/2}, x_{i+1/2}]$ where $x_{j+1/2} = \frac{x_j + x_{j+1}}{2}$ with $x_j = j\Delta x$.

A standard conservative formulation for (11) writes, in its first order version,

$$u_i^{n+1} = u_i^n - \lambda\Big(\hat{f}(u_i^n, u_{i+1}^n) - \hat{f}(u_{i-1}^n, u_i^n)\Big) \tag{12}$$

with $\lambda = \Delta t/\Delta x$. The second order predictor corrector scheme we use is

$$u_i^{n+1/2} = u_i^n - \frac{\lambda}{2}\Big(\hat{f}(u_{i+1/2}^{n,L}, u_{i+1/2}^{n,R}) - \hat{f}(u_{i-1/2}^{n,L}, u_{i-1/2}^{n,R})\Big) \tag{13a}$$

$$u_i^{n+1} = \frac{u_i^n + u_i^{n+1/2}}{2} - \lambda\Big(\hat{f}(u_{i+1/2}^{n+1/2,L}, u_{i+1/2}^{n+1/2,R}) - \hat{f}(u_{i-1/2}^{n+1/2,L}, u_{i-1/2}^{n+1/2,R})\Big) \tag{13b}$$

where

$$u_{j+1/2}^R = u_j + \delta_j/2, \qquad u_{j-1/2}^L = u_j - \delta_j/2$$

and $\delta_j = \mathcal{L}(u_{j+1} - u_j, u_j - u_{j-1})$ and $\mathcal{L}$ is a standard limiter. In this paper, we have chosen the superbee limiter,

$$\mathcal{L}(a, b) = \max\big(0, \min(2a, b), \min(a, 2b)\big).$$

The flux is the Murman–Roe flux with Harten's entropy fix for the Burgers equation,

$$\hat{f}(a, b) = \frac{1}{2}\Big(f(a) + f(b) - \lambda(a, b)(b - a)\Big) \tag{14}$$

where, if $\tilde{f}'(a,b)$ is the Roe average,

$$\lambda(a,b) = \begin{cases} |\tilde{f}'(a,b)| & \text{if } |\tilde{f}'(a,b)| > \varepsilon \\ \dfrac{|\tilde{f}'(a,b)|^2 + \varepsilon^2}{2\varepsilon} & \text{else.} \end{cases}$$

Here, we have taken $\varepsilon = 0.01$.

We have also run a case where $S(x) = (\sin^2(x))'$. Here, the flux in (14) is modified by replacing $f(a)$ and $f(b)$ by

$$f(a) - \sin^2(x_a), \qquad f(b) - \sin^2(x_b)$$

where x_a and x_b are the physical locations of the unknown a and b, i.e.

$$\hat{f}(a,b) = \frac{1}{2}\Big(f(a) + f(b) - \lambda(a,b)(b-a)\Big) - \frac{1}{2}\Big(\sin^2(x_a) + \sin^2(x_b)\Big). \tag{15}$$

Assume now that the initial condition, though still periodic of period 2π depends on a random parameter. Each of (12), (13a) and (13b) is similar, so we concentrate on (12). We have again, for any physical cell $[x_{i=1/2}, x_{i+1/2}]$ and any Ω_j,

$$E(u_i^{n+1}|\Omega_j) = E(u_i^n|\Omega_j) - \lambda\Big(E\big(\hat{f}(u_{i+1/2}^{n,L}, u_{i+1/2}^{n,R})|\Omega_j\big) - E\big(\hat{f}(u_{i-1/2}^{n,L}, u_{i-1/2}^{n,R})|\Omega_j\big)\Big) \tag{16}$$

This amounts to computing the flux expectancies, $E\big(\hat{f}(u_{i+1/2}^{n,L}, u_{i+1/2}^{n,R})|\Omega_j\big)$. For this, again, we reconstruct the variables $u_{i+1/2}^{n,L}$ and $u_{i+1/2}^{n,R}$ with the technique of section 3.1. In the numerical examples, we have either used a third order accurate centered reconstruction or the second order ENO one in the probability direction. As expected, the centered reconstruction generates (slight) oscillations. We only display the results with the ENO one. In the probability dimension, we use a Gaussian quadrature formula with two points. Hence, if we have N_{prob} cells in the probability direction, we need $2N_{prob}$ solution evaluations. The time step, i.e. λ is chosen by a worst case scenario, but this strategy might be over pessimistic. Further studies are certainly needed.

6.1 Convection problem

The example is the convection equation (velocity of unity) with an initial condition u_0. Since the exact solution is $u(x,t) = u_0(x-t)$ it is easy to evaluate the error on the mean and the variance. In the example, the pdf is $\mathcal{N}(1,1)$. In figure 5, we have displayed the results for 11, 21 and 41 points in the probability space. The results are second order accurate in space. We have also displayed the same results but for a Gaussian law with the same mean and the variance $\sigma = 0.1$. In that case, the gradient of the pdf is larger and then the quadrature formula (two point Gaussian) is less efficient. This could be improved by an adapted mesh, i.e. a mesh where the measure, with respect to the probability law, of each probability cell would be the same [12]. However, the results of Figure 6 indicate the same type of errors. This is confirmed by figure 7 where the same case are rerun with a fixed number of mesh points and 11 to 41 points in the probability space. Note that the same example gives, in the deterministic case, the following errors : $0.799\,10^{-2}$ in the max norm and $0.7919\,10^{-3}$ for the L^2 norm. This shows that the main source of error comes from the space discretisation, as in the elliptic case.

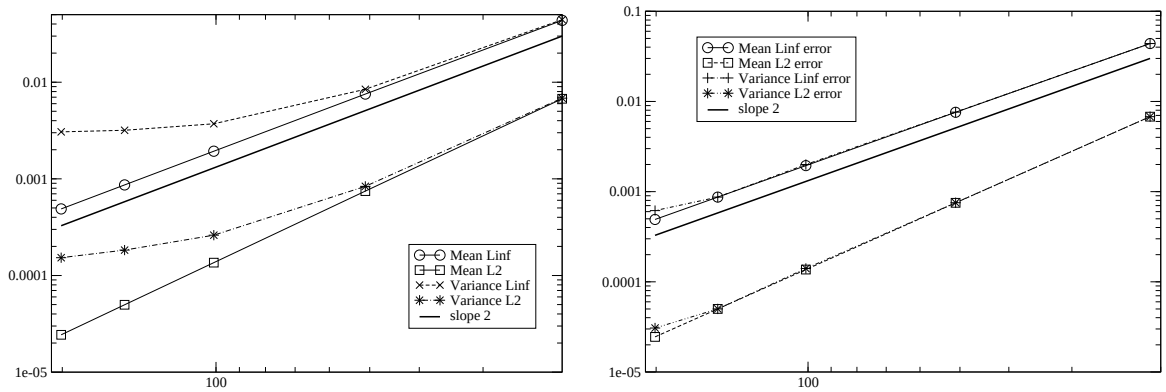

11 points in prob space

21 points in prob space

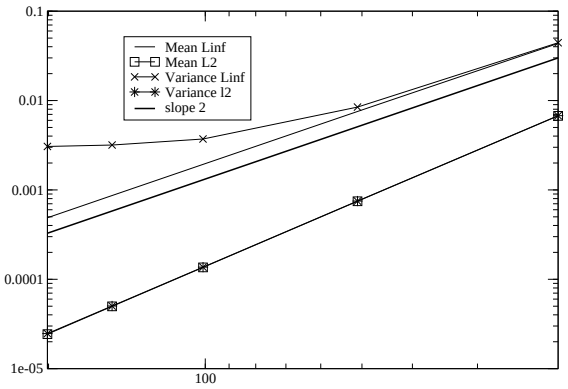

41 points in prob space

Figure 5: Errors in mean and variance for the convection problem with the pdf $\mathcal{N}(1,1)$, the CFL number is 0.75. The final time is $t = 1.5$ and the domain is $[0, 2\pi]$. The slope limiter is center in the probability space.

6.2 Burgers equation

The initial condition is

$$u_0(x,\omega) = |a(\omega)| \sin(2x - a(\omega))$$

with $a(x) = x$. This results in a a discontinuous solution with a discontinuity localised at $x_\omega = a(\omega)$. Three pdfs were used:

1. A Gaussian pdf: $\mathcal{N}(m,\sigma)$ with $m = 1$ and $\sigma = 0.1$ or 1 conditioned by $x \in [-3,3]$.
2. A discontinuous pdf defined by $d\mu = \frac{f}{w}dx$ with

$$f(x) = \begin{cases} 0 & \text{if } x \leq -1 \\ 0.1 & \text{if } x \in]-1, 0.5[\\ 1 & \text{if } x \in [0.5, 1[\\ 0 & \text{if } x \geq 1 \end{cases}$$

and $w = 0.65$ (i.e. the weighting factor so that the integral of f/w is equal to 1.)

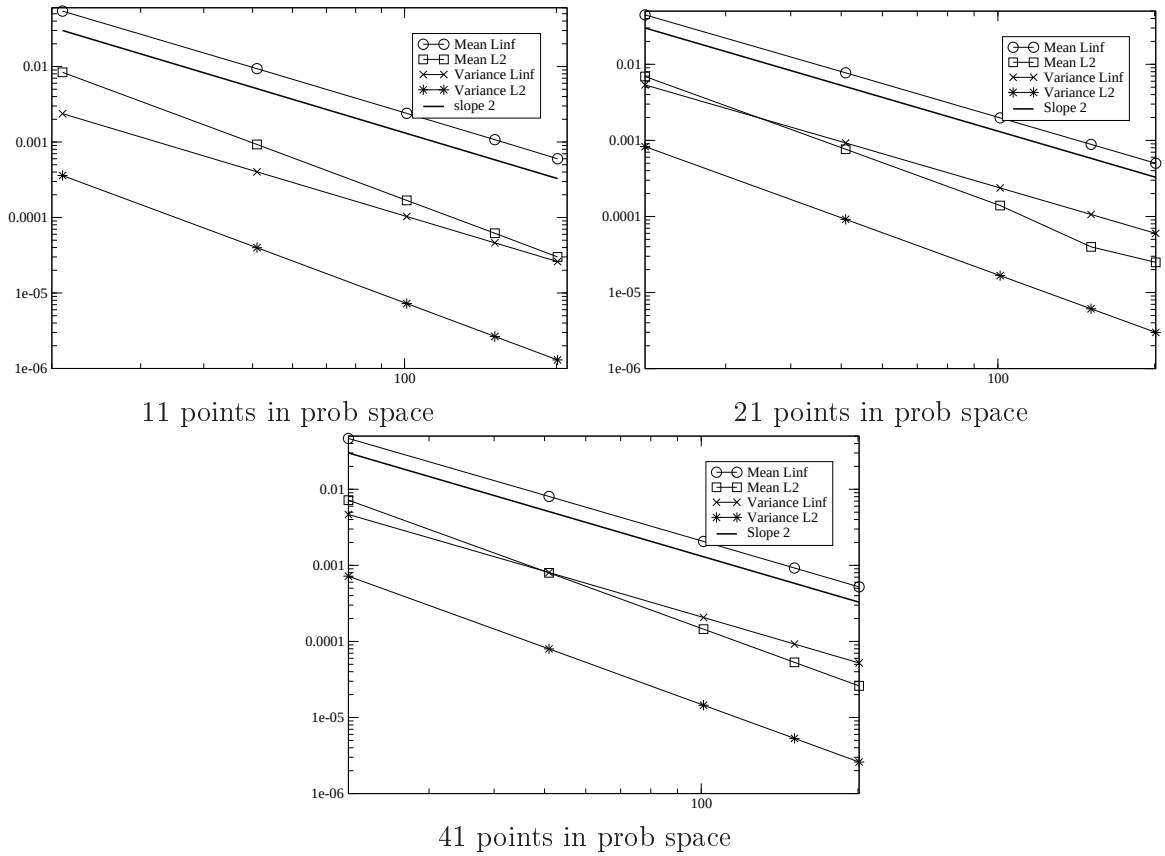

11 points in prob space

21 points in prob space

41 points in prob space

Figure 6: Errors in mean and variance for the convection problem with the pdf $\mathcal{N}(1, 0.1)$, the CFL number is 0.75. The final time is $t = 1.5$ and the domain is $[0, 2\pi]$. The slope limiter is centered in the probability space.

On Figure 8, we have represented for the two types of pdfs. The aim of this picture is to show the highly oscillatory behavior of the solution. To get them, we had to use the ENO–like limiter : the centered one produces oscillations as expected. In the case of the Gaussian pdfs, the realisations are the same, but their weights are different. Figure 9 is more interesting. We show, for each example, the mean, mean $\pm\sigma/2$ of the initial solutions and the computed solutions at time 1.5. The computations have been done with 101 space cells and 21 cells in the probability direction. Clearly the solutions are very different. One should not be surprised by the highly oscillatory behavior of the "Gaussian" solution with $\sigma = 1$. A close look at Figure 8 plus the understanding that the pdf is not very peaky in that case helps to understand that the weight of the discontinuities for amplitudes (and phases) near ± 3 play an important role in the evaluation of the means.

6.3 Burgers equation with source term

This example is taken from [5]. The initial condition is

$$u(x, 0) = \beta \sin x$$

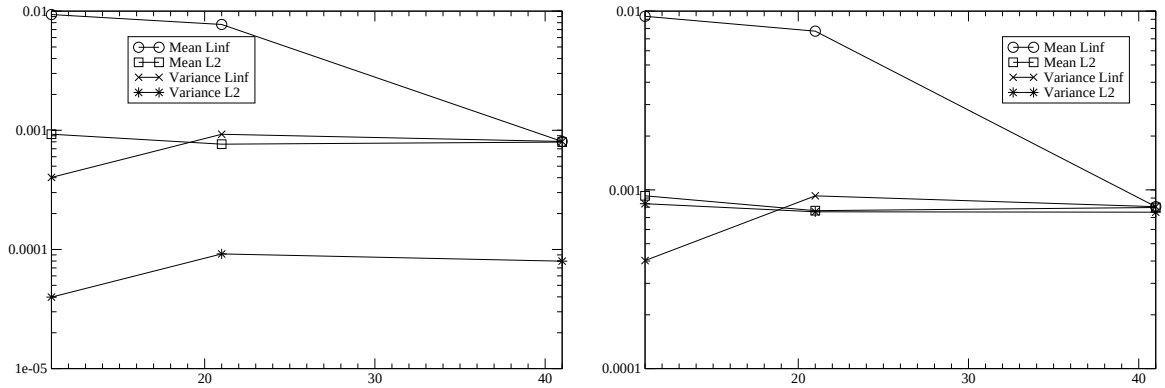

$\sigma = 0.1$ $\sigma = 1$

Figure 7: Errors in mean and variance for the convection problem with the pdf $\mathcal{N}(1, \sigma)$, $\sigma = 0.1$ and 1. The final time is $t = 1.5$ and the domain is $[0, 2\pi]$, the CFL number is 0.75 and there are 51 mesh points. The slope limiter is centered in the probability space.

with periodic boundary conditions on $[0, \pi]$. The exact steady solution is

$$u_\infty(x, \beta) = \lim_{t \to +\infty} u(x, \beta, t) = \begin{cases} u^+ = \sin x & \text{if } 0 \le x \le X_s \\ u^- = -\sin x & \text{if } X_s \le x \le \pi \end{cases}$$

where the shock location is

$$X_s = \begin{cases} \arcsin \sqrt{1 - \beta^2} & \text{if } -1 < \beta \le 0 \\ \pi - \arcsin \sqrt{1 - \beta^2} & \text{if } 0 < \beta \le 1 \end{cases}$$

If $|\beta| \ge 1$, the solution is smooth.

In [5] is considered the case of β random where $\alpha = \dfrac{\beta}{1 - \beta^2}$ is Gaussian with mean m and variance σ. We have

$$\beta = \begin{cases} \dfrac{-1 + \sqrt{1 + \alpha^2}}{2\alpha} & \text{if } \alpha \neq 0 \\ 0 & \text{else.} \end{cases}$$

We see that β defined as this is always in $[-1, 1]$, so a shock always exists. The density of the shock location is

$$p(x) = \begin{cases} \dfrac{1}{\sigma\sqrt{2\pi}} \dfrac{1 + \beta^2}{(1 - \beta^2)^2} e^{-[(x-m)^2/2\sigma^2]} \sin(x) & \text{if } x \in [0, \pi], \\ 0 & \text{else} \end{cases}$$

In the numerical section, we are going to evaluate the repartition function $x \mapsto P_{\sigma,m}(X_x \le x)$. An easy calculation shows that

$$P_{\sigma,m}(x) = P(X_s \le x) = \frac{1}{\sigma\sqrt{2\pi}} \int_{-\infty}^{-\frac{cosx}{\sin^2 x}} e^{-\frac{(x-\mu)}{2\sigma^2}} dx = \begin{cases} \operatorname{erf}(-\frac{\frac{cosx}{\sin^2 x} - m}{\sigma\sqrt{2}}) & \text{if } 0 \le x \le \frac{\pi}{2} \\ \frac{1}{2} + \operatorname{erf}(-\frac{\frac{cosx}{\sin^2 x} - m}{\sigma\sqrt{2}}) & \text{if } \frac{\pi}{2} \le x \le \pi \end{cases}$$

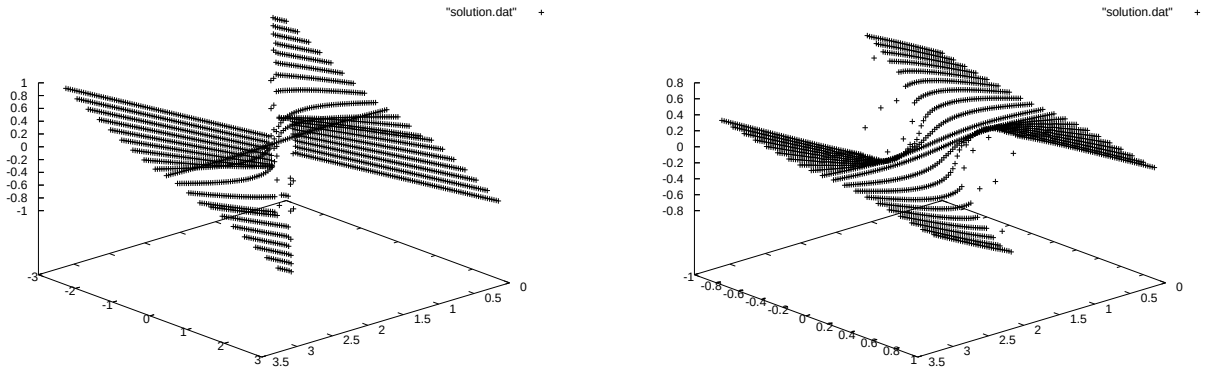

with the Gaussian pdfs with the discontinuous pdf

Figure 8: Plot of each realisation for the Gaussian pdfs and the discontinuous one.

In order to show the flexibility of the method, we also consider the sum of the previous pdf and a Dirac measure. More precisely,

$$d\mu = \frac{1}{I}\left(\frac{1}{\sigma\sqrt{2\pi}}e^{-[(x-m)^2/2\sigma^2]}1_{[A,B]}dx + \theta\delta_{\omega_c}\right) \tag{17a}$$

where $\omega_c \in]A,B[$, $\theta \geq 0$, I is the normalizing factor

$$I = \int_A^B \frac{1}{\sigma\sqrt{2\pi}}e^{-[(x-m)^2/2\sigma^2]}dx + \theta. \tag{17b}$$

and δ_{ω_c} is the Dirac distribution at $\omega = \omega_c$. In that case, the repartition function is

$$P_\mu(x) = P_{\sigma,m}(x) + \theta 1_{[Y,B]}$$

where Y is the shock location for $\alpha = x_c$, i.e.

$$Y = \pi - \arcsin\left(\sqrt{1-\beta^2}\right), \qquad x_c = \frac{\beta}{1-\beta^2}.$$

The simulation is initialised with, in each cell, the expectancy of the spatial averaged solution. The solution develops shocks. Since the method is a finite volume one, these shocks are at best known with an accuracy of $O(\Delta x)$. We have adopted the following procedure to localize the shock position: for each cell $[\omega_{j-1/2}, \omega_{j+1/2}]$, we determine the cell $]x_{i_j-1/2}, x_{i_j+1/2}[$ such that

$$\left|\frac{E(u_{i+1}|\Omega_j) - E(u_i|\Omega_j)}{\Delta x}\right|$$

is maximal. If this occurs at two different locations, we choose the smallest index. Once the index i_j is known, we compute

$$p(x_{i_j}) = P(x \leq x_{i_j})$$

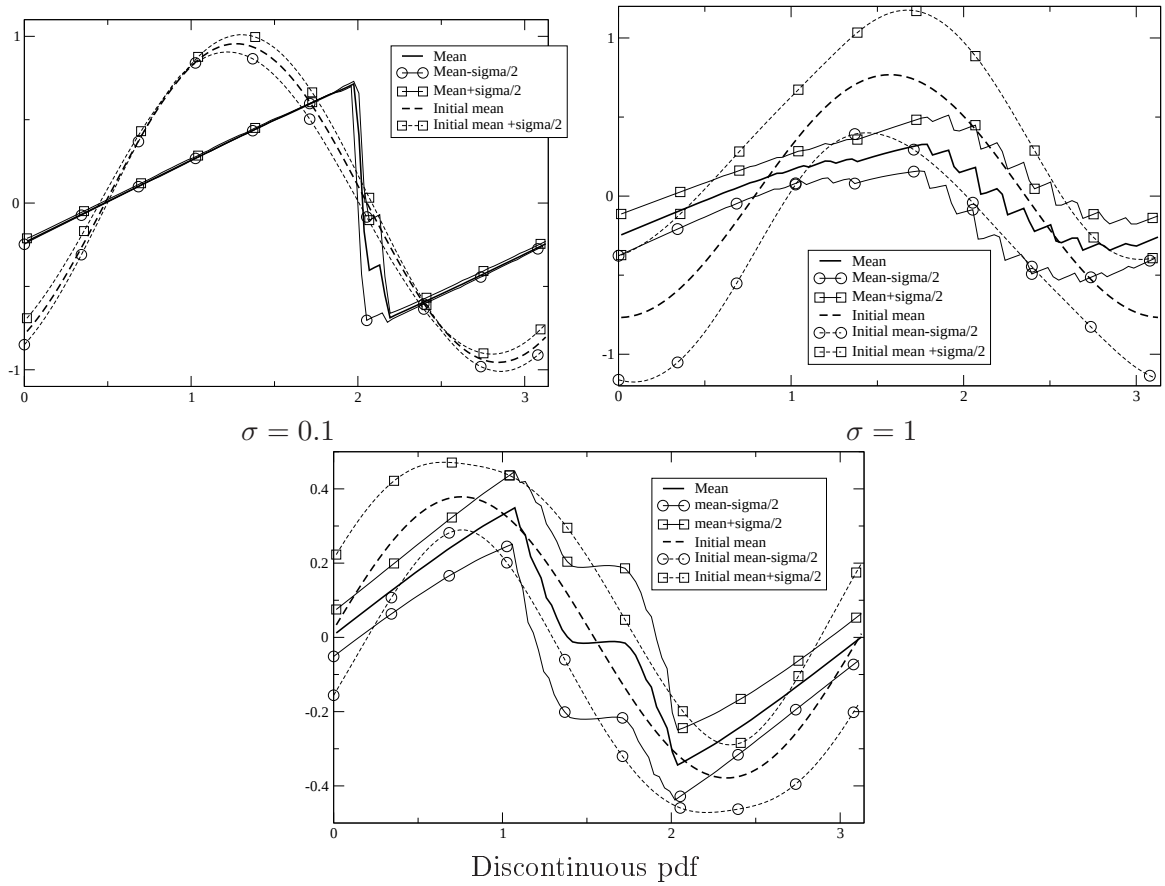

Figure 9: Means and mean $\pm\frac{\sigma}{2}$ for each pdf.

Note that for many j, $|i_j - i_{j+1}| > 1$: this means that there are "holes" in the numbering since the shock detection procedure may well decide that for j and $j+1$, the shock has the same location. See figure 10 for an illustration. It order to fill these gaps and to be able to draw $x_i \mapsto p(x_i)$, we make a linear interpolation between two consecutive gaps. The numerical repartition function is compared to the exact repartition one, and to the repartition function computed for the exact shock locations corresponding to the events $\frac{\omega_l+\omega_{l+1}}{2}$, $l = 1, \cdots$.

In the first set of example, we have considered a Gaussian distribution with $m = 1$ and $\sigma = 1$ for 101 and 151 mesh points in space, and 5 and 11 points in the probability direction. This corresponds to 100 and 150 'space" cells and 4 and 10 "probability" cells. The point repartition is uniform in both directions. The results are displayed in Figure 11. A good agreement is obtained: remember that the shock locations are at most known with an $O(\Delta x)$ error. A close inspection of the figure indicates that for $x \approx \pi$, the numerical repartition function has a discontinuity which is not existing in the exact one. The explanation is the following: our variables are the expectancies of the averaged variables : $E(u_i|\Omega_j)$, which can be though as the value of u_i at $\omega_{j+1/2} = \frac{\omega_j+\omega_{j+1}}{2}$. Hence, the shock location for this random parameter does not correspond to the random parameter α for which $x_l = \arcsin\left(\sqrt{1-\beta^2(\alpha)}\right)$. The difference is the most visible for the first row. This is

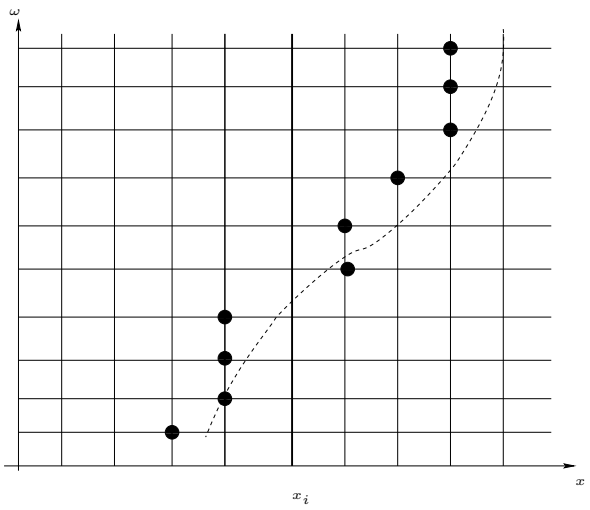

Figure 10: Illustration of the shock location mechanism. The theoretical shock location is represented by the dotted curve. The black spots are the shock locations. Consider the thick vertical line : there is a jump of $2\Delta x$ when going to ω_j to ω_{j+1} so that there is no ω_l for which x_i corresponds to a shock for the realisations in $[\omega_l, \omega_{l+1}]$.

why we have also plotted the exact value of the repartition function for the $\omega_{j+1/2}$. We also see a jump, and the agreement is now very good.

The Figure 12 represents the same type of results for the singular pdf (17). Here $\theta = 1$ and $\omega_c = 0.5$. This corresponds to the shock location $x_c \approx 1.997874914$. The same comments as in the previous examples can be given.

7 Example of the Euler equations

The method is easily extended to the Euler equations. The base scheme is the second Roe scheme using the superbee limiter on the characteristic variables. We use the wave interpretation of the Roe scheme to construct the second order scheme (see [13]). Even-though the scheme use the conservative variables $W = (\rho, \rho u, E)$ for the time evolution, the main variables are the density ρ, the velocity u and the pressure p. The total energy is related to these variable via an equation of state. Here, we have chosen a perfect gas EOS,

$$E = \frac{p}{\gamma - 1} + \frac{1}{2}\rho u^2,$$

where the ratio of specif heats γ may be non uniform. In that case, we use the version of the Roe scheme developed in [14]. Examples of this type have been successfully run, but are not reported here.

In order to show the versatility of our method, we have run the method on two classes of examples, namely a shock tube like problem, and the interaction of a density sine wave with a shock (as proposed by Shu and Osher).

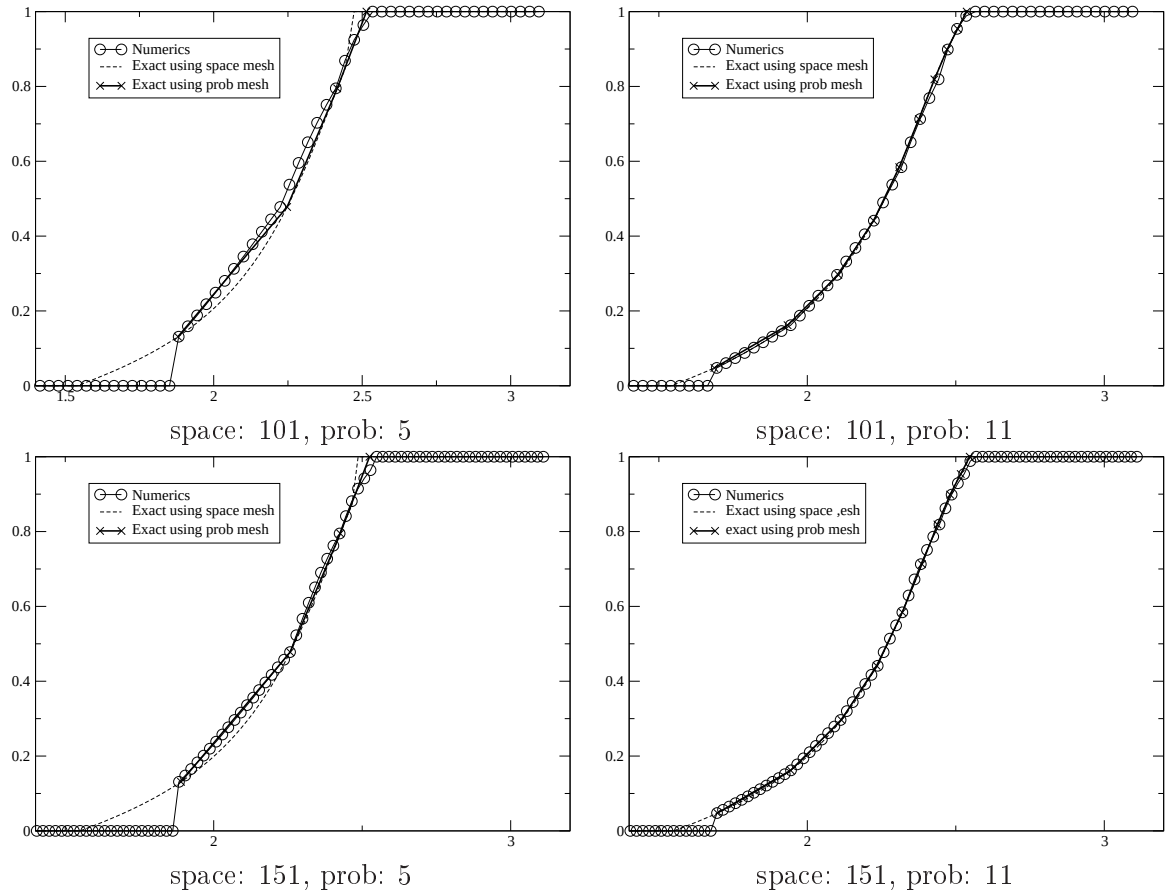

Figure 11: Solution for the double nozzle problem obtained with the Gaussian law. Numeric : distribution obtained from the solver. Exact : exact distribution. Exact from prob mesh : distribution at the points $\omega_{j+1/2}$.

The uncertainty parameters are now two dimensional, and in the examples we show, we have chosen a Gaussian type law where the uncertainty are correlated. The pdf is

$$f(\omega_1, \omega_2) = Ke^{-\frac{\omega_1^2 - (\omega_2 - 1)^2 - \omega_1(\omega_2 - 1)}{2}}, \tag{18}$$

and K is a normalizing coefficient and $(\omega_1, \omega_2) \in [-3, 3]^2$.

7.1 Shock tube like test cases

The initial conditions are

- If $x \leq 0.5$,

$$\begin{aligned} \rho(x) &= \rho_L(1 + 0.2\sin(\omega_1)) \\ u(x) &= u_L \\ p(x) &= p_L(1 + 0.2\sin(\omega_2)) \end{aligned}$$

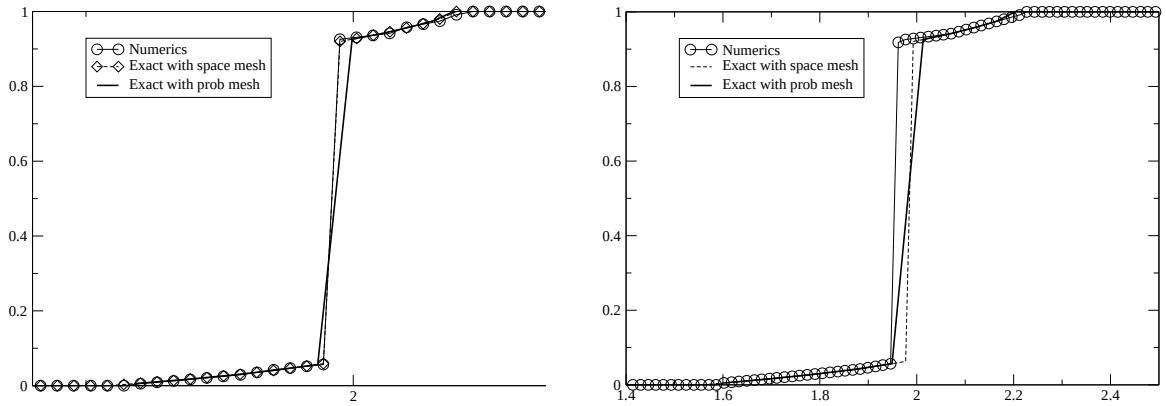

space: 101, prob: 11 space: 201, prob: 11

Figure 12: Solution for the double nozzle problem obtained with the law (17). Numeric : distribution obtained from the solver. Exact : exact distribution. Exact from prob mesh : distribution at the points $\omega_{j+1/2}$.

- else

$$\begin{aligned}\rho(x) &= \rho_R(1 + 0.2\sin(\omega_1))\\ u(x) &= u_L\\ p(x) &= p_R(1 + 0.2\sin(\omega_2))\end{aligned}$$

with $\gamma = 1.4$. The density of the random variables ω_1 and ω_2 is given by (18). The CFL condition is set to 0.75. The results are displayed in Figure 14. Again several resolution in the probability directions have been run. Again, we see that the results, on that case, are indistinguishable.

7.2 Shock-turbulence interaction

The initial conditions are, with $\rho_L = 3.857143$, $u_L = 2.629369$, $p_L = 10.333333$ and $u_R = 0.$, $p_R = 1.$, and $s_{loc} = -4$,

- If $x \leq s_{loc}$,

$$\begin{aligned}\rho(x) &= \rho_L\\ u(x) &= u_L\\ p(x) &= p_L\end{aligned}$$

- else

$$\begin{aligned}\rho(x) &= 0.5\ (1 + 0.2\sin(5x))\\ u(x) &= u_R\\ p(x) &= p_R(1.0 + 0.2\sin(\omega_1 + \omega_2))\end{aligned}$$

On figure 14, the simulation is done with 400 points in the space direction and 10×10 or 20×20 in the probability space. Again the same conclusion holds: there is little dependency on the probability direction resolution.

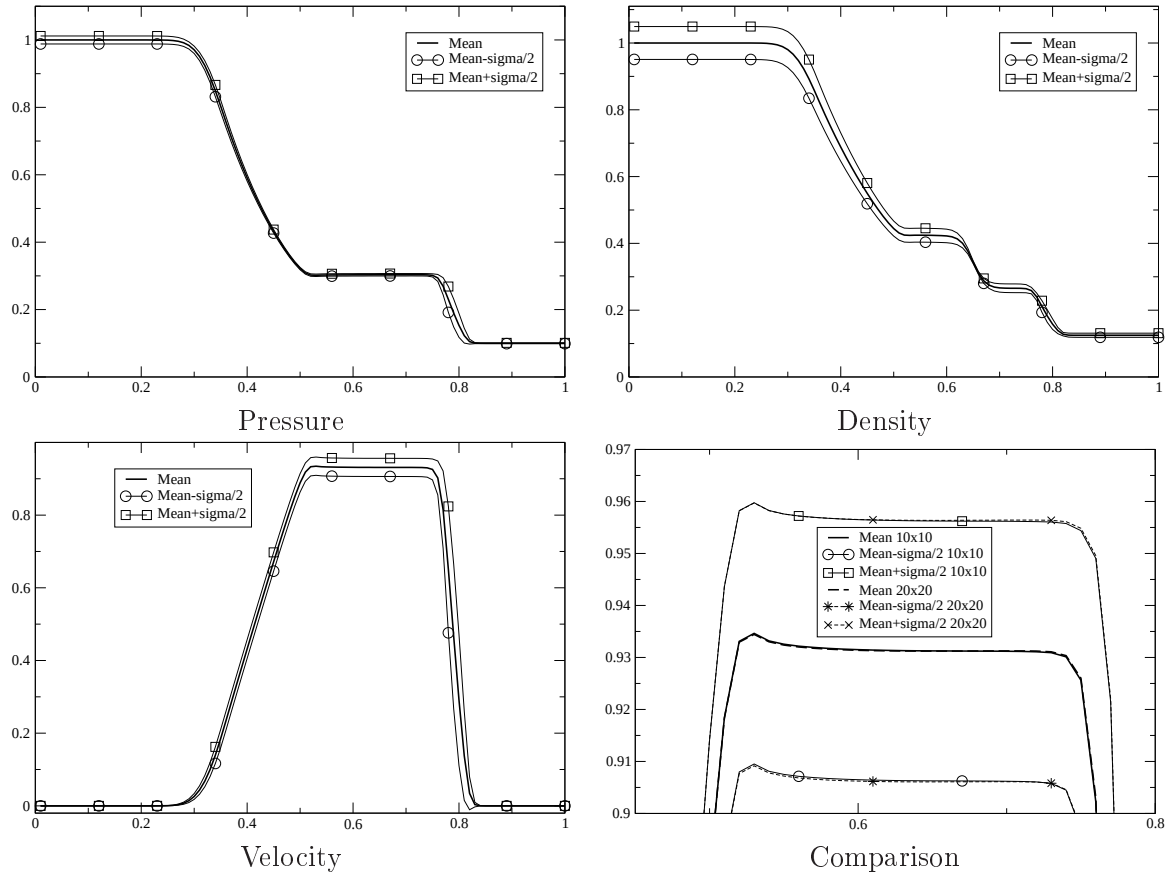

Figure 13: Sod tube case with random densities and pressure. Two correlated random variables are used.

8 CPU considerations

For several of the previous problems, we give on table 2 the CPU cost obtained on a MacBook Pro running at 2.4 Ghz with 2Go of ram and the Intel (10.1) compiler (no option). No particular optimisation has been performed. This table show that the CPU is rather low.

9 Conclusions

We have described and illustrated a general method that enable to compute some statistics on the solution of a PDE or and ODE, linear and non linear. The source of uncertainty may be multidimensional. The technique relies on a reconstruction method in the random variable. This reconstruction technique is standard in finite volume scheme, except that the measure is no longer the Lebesgue measure but is the probability law. This method enable to consider random variable that depend on possibly correlated random variables. The solution description uses the expectancies of a given function conditioned by the belonging of the random variable to subsets that are mutually in dependant and covers Ω.

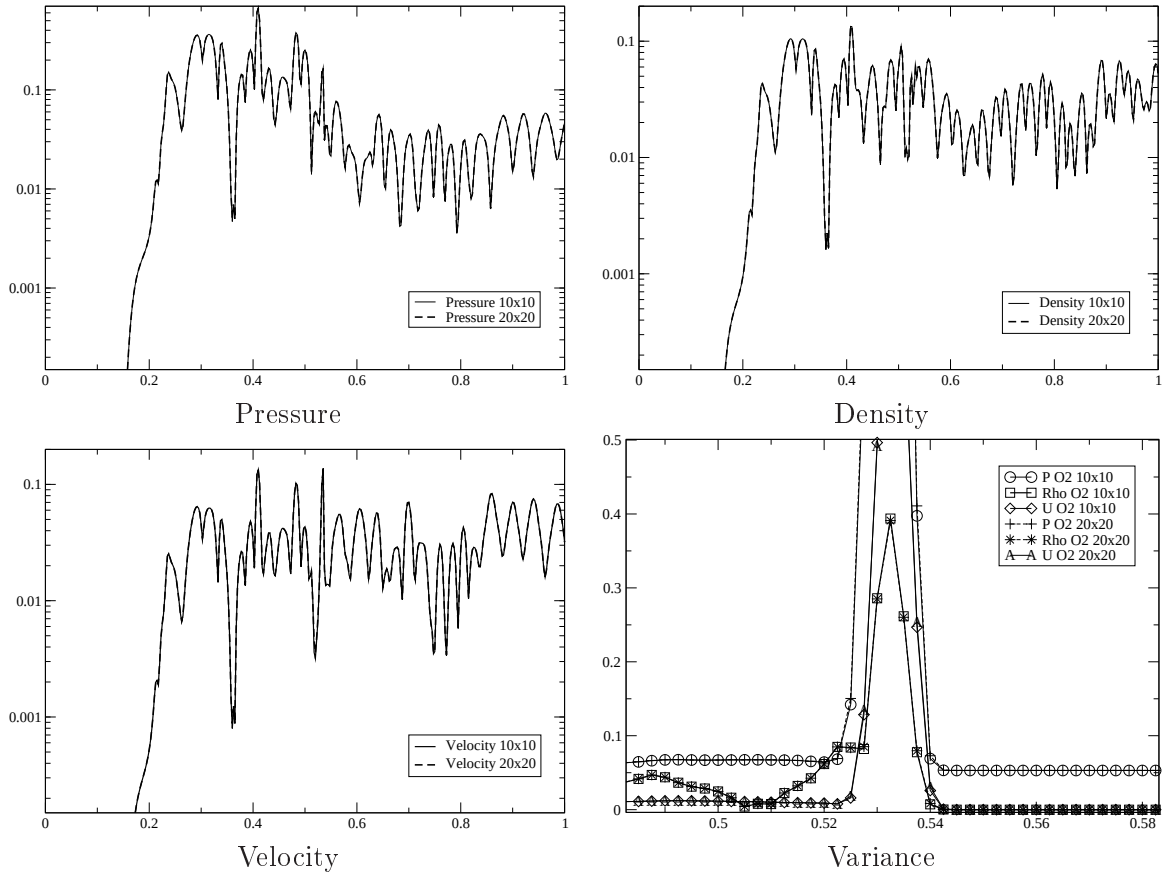

Figure 14: Shu and Osher case with a random post shock state. Two correlated random variables are used.

Given one problem and an integration method, we have shown how to construct a scheme which enable to approximate these conditional expectancies.

The method is illustrated on several types of problems, linear and non linear, including the Euler equations. The method is cheap and flexible. Its accuracy is linked to the accuracy of the reconstruction and the deterministic solution method. We show numerically that the main sources of errors are still in the deterministic scheme. Correlated source of uncertainties can easily be implemented in this framework, as well as very general pdfs.

In a future work, we will extend this to the Navier Stokes equations, see how the case of many random variables can be handled in this framework. Note that [15], using a related method, has already considered turbulence problems with one or two sources of uncertainties.

References

[1] R.H. Cameron and W.T. Martin. The behavior of measure and measurability under change of scale in Wiener space. *Bull. Am. Math. Soc.*, 53:130–137, 1947.

Problem	number of points (space)	number of points (prob)	CPU
Burgers Nozzle	101	11	10s
Burgers Nozzle	201	11	43s
Burgers	101	11	0.8s
Burgers	201	11	3s
Euler 2(Shu-Osher)	200	20x20	152s

Table 2: CPU cost for several problems. The stopping criteria are : iterative convergence 10^{-6} for the steady nozzle ; Burgers: final time $t = 1$; Euler equations with 2 uncertainties: final time : 1. The pdfs are Gaussian.

[2] X. Wan and G. E. Karniadakis. Beyond Wiener-Askey expansions: handling arbitrary PDFs. *J. Sci. Comput.*, 27(1-3):455–464, 2006.

[3] X. Wan and G. E. Karniadakis. Multi-element generalized polynomial chaos for arbitrary probability measures. *SIAM J. Sci. Comput.*, 28(3):901–928, 2006.

[4] B. J. Debusschere, H. N. Najm, P. P. Pébay, O. M. Knio, R. G. Ghanem, and O. P. Le Maître. Numerical challenges in the use of polynomial chaos representations for stochastic processes. *SIAM J. Sci. Comput.*, 26(2):698–719, 2004.

[5] D. Xiu and J. S. Hesthaven. High-order collocation methods for differential equations with random inputs. *SIAM J. Sci. Comput.*, 27(3):1118–1139, 2005.

[6] O.P. Le Maître, H.N. Najm, R.G. Ghanem, and O.M. Knio. Multi-resolution analysis of Wiener-type uncertainty propagation schemes. *J. Comput. Phys.*, 197(2):502–531, 2004.

[7] A. Harten, B. Engquist, S. Osher, and S. Chakravarthy. Uniformly high order accurate essentially non-oscillatory schemes. III. *J. Comput. Phys.*, 71:231–303, 1987.

[8] Timothy J. Barth and Paul O. Frederickson. Higher order solution of the euler equations on unstructured grids using quadratic reconstruction. AIAA paper 90-0013, January 1990.

[9] R. Abgrall. On essentially non-oscillatory schemes on unstructured meshes: Analysis and implementation. *J. Comput. Phys.*, 114(1):45–58, 1994.

[10] R. Abgrall and Thomas Sonar. On the use of Mühlbach expansions in the recovery step of ENO methods. *Numer. Math.*, 76(1):1–25, 1997.

[11] P. Lesaint and P.A. Raviart. On a finite element method for solving the neutron transport equation. Math. Aspects finite Elem. partial Differ. Equat., Proc. Symp. Madison 1974, 89-123 (1974)., 1974.

[12] T.J. Barth. Private communication, may 2008.

[13] R.J. LeVeque. *Finite volume methods for hyperbolic problems.* Cambridge University Press, 2002.

[14] R. Abgrall and Smadar Karni. Ghost-fluids for the poor: a single fluid algorithm for multifluids. In *Hyperbolic problems: theory, numerics, applications, Vol. I, II (Magdeburg, 2000)*, volume 141 of *Internat. Ser. Numer. Math., 140*, pages 1–10. Birkhäuser, Basel, 2001.

[15] T.J. Barth. Deterministic propagation of model parameter uncertainties in compressible navier-stokes calculations. 6th International Conference on Engineering and Computational Technology, Athen, September 2008.